Acta Scientiarum

http://www.periodicos.uem.br/ojs/
ISSN on-line: 1807-863X
Doi: 10.4025/actascibiolsci.v43i1.57856





# *In vitro* and *in vivo* genotoxicity and cytotoxicity analysis of protein extract from *Aplysina fulva* sponges

**Alan de França Santana[1], Ingrid Regina Avanzi[1], Julia Risso Parisi[2], Matheus Almeida Cruz[1], Giovanna Caroline Aparecida do Vale[1*], Tiago Akira Tashiro de Araújo[1], Samuel Rangel Cláudio[1], Daniel Araki Ribeiro[1], Renata Neves Granito[1] and Ana Claudia Muniz Renno[1]**

[1]Departamento de Biociências, Universidade Federal de São Paulo, Rua Silva Jardim 136 - Vila Matias, 11015-020, Santos, São Paulo, Brazil. [2]Departamento de Fisioterapia, Universidade Federal de São Carlos, São Carlos, São Paulo, Brazil. *Author for correspondence. E-mail: gica.vale@hotmail.com

**ABSTRACT.** This study evaluated the physicochemical and morphological properties of a marine sponge protein extract (PE) using scanning electron microscopy (SEM), Energy dispersive X-ray spectroscopy (EDS), analysis of mass loss and pH and *in vitro* and *in vivo*. Scanning electron microscopy showed that PE fibers present a granular aspect and irregular structure and the element carbon followed by oxygen was detected in the EDS analysis. Moreover, a 29% of mass loss was observed after 14 days and the pH slightly modified after 14 days. Cell viability of fibroblast cells (L929) of control and PE at a concentration of 25% demonstrated higher values compared to the groups. Osteoblast cell viability of PE at 25 and 50% was significantly higher. Comet assay on day 1 showed higher values for PE at 25%. In addition, *in vivo* experiments demonstrated that in the treated animals, the bone defects were filled with biomaterial particles, granulation tissue and some areas of newly formed bone. Furthermore, similar immunoexpression of Runx-2 and Cox-2 was observed. Taken together, all results suggest that PE is biocompatible, present non-citotoxicity in the *in vitro* studies (at the lower concentration) and in the *in vivo* studies and it can be considered as an alternative source of collagen for tissue engineering proposals.

**Keyword:** biomaterials; marine sponge; protein extract, biocompatibility; marine biodiversity.

Received on February 18, 2021.
Accepted on April 23, 2021.

## Introduction

Collagen (Col) has been frequently used as a biomaterial for tissue engineering proposals especially as bone grafts, skin membranes and therapeutic enzymes immobilization (Davison-Kotler, Marshall, & García-Gareta, 2019). Natural Col can be derived from tissues of different species but primarily from bovine and porcine skin and bones (Khan & Khan, 2013). However, the process of extraction and purification of this type of Col is complex and expensive (Colchester & Colchester, 2013). Also, the use of mammalian Col involves some health issues such as the transmission of diseases (bovine spongiform encephalopathy and foot-and-mouth disease) as well as religious constraints (Cicciù et al., 2018). In this context, marine Col has been emerging as a promising alternative to substitute the standard sources of Col (Chattopadhyay & Raines, 2014; Silva et al., 2014).

Marine Col can be obtained from fishes, crustaceous, invertebrate animals such as sea anemone, prawns, jellyfish and more recently, sponges (Lim, Ok, Hwang, Kwak, & Yoon, 2019; Felician, Xia, Qi, & Xu, 2018) Marine sponges (phylum Porifera) are one of the most promising species of biological elements and molecules, with a vast potential for a wide range of applications mainly due to the antitumor, antiviral and anti-inflammatory effects of their biocompounds (Wang et al., 2009; Müller et al., 2002). Marine sponges are sessile animals considered representatives of the first multicellular animals and their structure and composition are formed by many bioactive components including marine Col (also known as spongin (SPG) or protein extract (PE)) (Green, Lee, & Jung, 2015; Iwatsubo, Kishi, Miura, Ohzono, & Yamaguchi, 2015; Green, Howard, Yang, Kelly, & Oreffo, 2003; Hoyer et al., 2012). Protein extract is very similar to human Col type XIII, with hydrophobic transmembrane domains and with binding properties, being able to stimulate cellular adhesion, migration and cytoskeletal organization (Hägg et al., 2001; Ylönen et al., 2005).

Furthermore, PE presents specific chemical and mechanical properties such as lower viscosity at a given concentration, lower water solubility and lower proportions of proline compared to those observed in mammalian Col, which makes it more suitable for tissue engineering applications (Lim et al., 2019; Pozzolini et al., 2018). For example, Pozzolini et al., (2018) manufactured a skin membrane for treating burns using PE from marine sponges (*C. reniformis*) and observed that this material showed good mechanical properties, antioxidant activity and biocompatibility on both fibroblast and keratinocyte cell cultures (Pozzolini et al., 2018). Parisi et al. (2019), in an *in vitro* study, observed a significant increase of fibroblast and osteoblast cell viability seed onto PE and hydroxyapatite *scaffolds*.

Despite the positive evidences of PE towards the stimulation of cells, no study investigating the morphological characteristics, genotoxicity and cytotoxicity of this compound has been performed yet. Thus, our hypothesis is that PE is biocompatible and may constitute a possible alternative substrate for tissue engineering applications. Consequently, our aim was to investigate the physicochemical and morphological properties of PE by using scanning electron microscopy (SEM), Energy dispersive X-ray spectroscopy (EDS), mass loss and pH. Moreover, the cytotoxicity and genotoxicity of PE were studied using *in vitro* (cell viability and comet assay) and *in vivo* studies using a model of bone defect in rats.

## Material and methods

### Reagent/Materials

The reagents used in this study are described below: EDTA (Labsynth Products Laboratories, Diadema, Brazil), urea Labsynth Products Laboratories, Diadema, Brazil), Tris-HCl (Labsynth Products Laboratories, Diadema, Brazil), NaOH (Labsynth Products Laboratories, Diadema, Brazil), 2-mercaptoethanol (Sigma-Aldrich, St. Louis, The United States) and acetic acid (Labsynth Products Laboratories, Diadema, Brazil). A commercial bovine collagen (US Biological Life Sciences, Salem, The United States) was used as a comparative group for PE in the *in vitro* studies. Also, materials were packaged and sterilized by ethylene oxide (Acecil, Campinas, SP, Brazil).

### PE extraction

*Aplysina fulva* marine sponge was used for the PE extraction. Samples were collected in Praia Grande (23º49'23.76 "S, 45º25'01.79" W, São Sebastião, Brazil) and in the area of Araçá Bay (23º81'73.78 "S, 45º40'66.39 "W, São Sebastião, Brazil). Protein extract extraction was performed based on the methodology of Swatschek, Schatton, Kellermann, Müller, and Kreuter (2002). Samples of sponges were collected from nature using a scalpel blade and were transported to the laboratory in thermal boxes (with sea water). Afterwards, species were washed with Milli-Q water for debris removal, cut in small pieces and placed separately in Tris-HCl buffer (100 mM, pH 9.5, 10 mM EDTA, 8 M urea, 100 mM 2-mercaptoethanol). After that, pH was adjusted to 9 with NaOH and solution was transferred into a stirred beaker for 24 hours. Solution was then centrifuged (5000 g; 5 minutes and 2 ºC), the pellet was discarded and the supernatant was removed. pH was adjusted to 4 and the precipitated was centrifuged again. The solution was lyophilized for preservation of the PE (Swatschek et al., 2002).

### Disk preparation

For this study, disks of PE and bovine Col (for mass loss and pH evaluation) were manufactured. The materials in powder were weighed and inserted in a 2 mL closed tip syringe (BD Plastipakt, Becton Dickinson S.A., Madrid, Spain) with distilled water. Subsequently, the syringe was connected in a mixing apparatus (Silamats, Vivadent, Schaan, Liechtenstein) and mixed for another 20s. Immediately after mixing, the material was injected into Teflon molds (Ø 3 mm x 1.8 mm). After overnight setting at room temperature, the pre-set disks were removed from the silicon molds.

### Material characterization
### Scanning electron microscopy (SEM)

Disks were mounted on aluminum stubs using carbon tape, sputter-coated with gold/palladium (System BAL-TEC MED 020, BAL-TEC, Liechtenstein) and examined by SEM using a ZEISS LEO 440 microscope (20 kV, 2.82 A).

### Degradation test and pH

To perform the degradation tests, samples were weighed, placed in 3 mL of phosphate buffered saline (PBS, 10mM, pH 7.4) in a Falcon tube and incubated at 37 °C in a water bath on a shaker table (70 rpm), for 3, 7 and 14 days. The assays were performed in triplicate (n=3). After the experimental periods, samples were analyzed.

Right after removal of the disks from the water bath, the pH of the PBS medium was measured. After the experimental periods, samples were removed from the Falcon tube and vacuum dried overnight before measuring the mass. Samples were weighed again and the difference between the initial and final mass was considered as the value of sample degradation.

### Cell culture studies

For the *in vitro* studies, calvarial osteoblast-like cells of rats (Osteo-1lineage) and murine fibroblasts (L929) were used in this study. These cell types were chosen based on the ISO 10993-3 and 10993-5 guidelines. Cell lines were cultured in bottles containing DMEM (L929) and α-MEM (MC3T3-E1) supplemented with 10% Bovine Fetal Serum (SFB), respectively, at 37 °C in humid atmosphere of 5% $CO_2$. Cells were maintained at subconfluent densities and passed every 2-3 days until use.

Cytotoxicity of PE and their influence on L929 and MC3T3 cell viability were assessed by an indirect assay using extracts of the materials (25, 50 and 100 mg $mL^{-1}$) above (Kido et al., 2013). Materials were sterilized by ultraviolet irradiation (UV) for 24 hours. The extracts were prepared according to the ISO 10993-5 and 10993-12, using as an extraction vehicle, the standard culture medium with de dilution described above. Then, samples were maintained for 24 hours in a humidified incubator set at 37 °C and 5% $CO_2$. After this period, culture medium containing the extracts was filtered using a 0.22 µm filter (Kasvi, Curitiba, Brazil). Extracts in the same concentration as the ones cited above, without the material, were used as control and incubated under the same conditions previously described (Kido et al., 2013). Subsequently, in the experimental periods of 3, 7 and 14 days, the alamarBlue® assay (Thermo Fisher Scientific, São Paulo, Brazil) was performed for all samples, at each time point for cell viability evaluation.

For this analysis, 500 µL of 10% alamarBlue® solution was added into each well and incubated in dark for 3 hours. After, 200 µL of solution (in duplicate) were aliquoted into the 96-well plates for analysis in the spectrophotometer (Bio-Tek Instruments, Inc.) at 570 and 600 nm. From the values obtained, the viability rate was calculated as the percentage reduction of alamarBlue®, according to the manufacturer's instructions (Parisi et al., 2019).

## Comet assay

Comet assay was performed in the osteoblast cell in the following experimental periods of 3, 7 and 14 days. The wells were washed with PBS and trypsin and, subsequently, cells were put into a 50 mL flask. Flasks were centrifuged (5 min. at 1200 rpm), the α-MEM medium was removed and 1 mL fresh α-MEM medium was added. Afterwards, 100 µL α-MEM was added to 120 µL 0.5% low melting-point agarose (Invitrogen, New York, USA) at 37 °C. Material was lightly placed in a 1.5 % agarose-precoated slide and covered with a coverslip. After agarose solidification inside the refrigerator, the coverslip was removed, and the slides were incubated (1 hour) in lysis solution [2.5 M NaCl, 100 mM EDTA (Merck, St. Louis), 10 mM Tris–HCl buffer, pH 10 (Sigma-Aldrich), 1 % sodium sarcosinate (Sigma-Aldrich), with 1 % Triton X-100 (Sigma-Aldrich) and 10 % dimethyl sulphoxide (Merck)]. Slides were immersed in alkaline buffer [0.3 mM NaOH (Merck) and 1 mM EDTA, pH > 13 (Merck)] for 20 min and the electrophoresis was performed (at 25 V, 0.86 V/cm and 300 mA) during 20 min. Afterwards, the slides were neutralized in 0.4 M Tris–HCl, pH 7.5, fixed in 100 % ethanol (Merck, Darmstadt, Germany) and stained (100 µL ethidium bromide, 50 mg $mL^{-1}$). The analysis of 50 comets/material/period was done at a magnification of ×400. A black and white camera mounted on a fluorescence microscope (Olympus, Orangeburg, USA) connected to an analysis software (Comet Assay II, Perceptive Instruments, Haverhill, Suffolk, UK) was used for examination. In order to measure the DNA damage, the tail moment was calculated: the comet tail moment is given by the product of the tail length and the fraction of DNA in the comet tail, consisting of the classification into categories (0 to 3), where 0 has no tail; 1 little; 2 intermediate, and 3 much tail, and it is positively related with the level of DNA damage in the cell. The tail moment mean value in a specific sample was assumed to be the index of DNA damage (Kido et al., 2013).

## *In vivo* study

### Material preparation

For the *in vivo* studies, disks of PE for bone defect implantation were made (3 mm diameter x 2 mm thick). Briefly, 1 g of PE powder was put into a 2 ml volume plastic syringe and 2 % $Na_2HPO_4$ solution was added. Afterwards, the syringe was placed in an amalgamator (Silamat, Vivadent, Schaan, Liechtenstein) and shaken for 20 seconds. The obtained mixture was placed into a Teflon mold (3 mm diameter x 2 mm thick), which dried overnight at 37 ºC. Disks were then removed from the Teflon molds and sent to sterilize with ethylene oxide (Acecil, Campinas, São Paulo, Brazil) and stored at room temperature (Parisi et al., 2019).

### Animals

For this experiment, 16 mature male Wistar rats (*Rattus norvegicus albinus*) were used (12 weeks, weight 300-350 g), distributed into 2 groups (n=8): control group (CG) and PE group (PE). All rats received one surgical procedure during the course of this experiment to induce a noncritical size bone defect in the right tibias. All animals were euthanized by anesthetic overdose after 7 days post-surgery. Animals were maintained in plastic cages, under controlled temperature (22 ± 2 ºC), light–dark periods of 12 hours and had free access to water and standard food (Gabbai-Armelin et al., 2015). This study was approved by the Animal Care Committee guidelines of the *Universidade Federal de São Paulo* (CEUA Nº5312090318).

### Surgical procedures

Noncritical size bone defects (3 mm diameter) were surgically created 10 mm below the articular joint of the right knee of the right tibia. Surgery was performed under sterile conditions and general anesthesia induced by intraperitoneal injection of 20 mg $kg^{-1}$ xilazin (Anasedan; Sespo Industry and Trade Ltda, Jacareí, SP, Brazil) and 40 mg $kg^{-1}$ ketamin (Dopalen; Sespo Industry and Trade Ltda, Jacareí, SP, Brazil). An incision was performed to expose the tibia and a standardized 3.0 mm diameter bone defect was created by using a motorized drill (Beltec®, Araraquara, SP, Brazil) under copious irrigation with saline solution. Subsequently, disks were implanted into the defects and the skin was sutured with resorbable polyglactin. The antisepsis was performed with povidone iodine and the animals were returned to their cages for recovering. The health status of the rats was monitored daily. Rats were euthanized 7 days post-surgery and the tibias were removed.

### Histopathological analysis

Samples were fixed in 10 % buffer formalin (Merck, Darmstadt, Germany) for 48 hours, decalcified in 4 % ethylenediaminetetraacetic acid (EDTA) (Merck, Darmstadt, Germany) and embedded in paraffin blocks. Thin sections (5 µm) were prepared perpendicularly to the medial-lateral drilling axis of samples using a microtome (Leica Microsystems SP 1600, Nussloch, Germany). Three sections of each specimen were stained with hematoxylin and eosin (Merck, Darmstadt, Germany) and examined using light microscopy (Leica Microsystems AG, Wetzlar, Germany, Darmstadt-Germany). The following parameters were evaluated: inflammatory process, granulation tissue, capsule formation, newly formed bone and the presence of the material in the area of the defect (Magri et al., 2019a; Garavello-Freitas et al., 2003). The analysis was performed by two observers (AFS and GCAV), in a blinded way.

### Immunohistochemistry

The immunoexpression of runt-related transcription factor-2 (Runx-2) and cyclooxygenase-2 (Cox-2) was determined using the streptavidin–biotin-peroxidase method (Magri et al., 2019a; Assis et al., 2013). Histological sections were deparaffinized using xylene and rehydrated in graded ethanol. Thereafter, the histological sections were pre-treated in a steamer with buffer Diva Decloaker (Biocare Medical, CA, USA) for 5 min. for antigen retrieval. The sections were pre-incubated with 0.3 % hydrogen peroxide (Labsynth, Diadema, Brazil) in PBS solution for 30 min in order to inactivate endogenous peroxidase and then blocked with 5 % normal goat serum in PBS solution for 20 min. Three sections of each specimen were incubated for 2 hours with polyclonal primary antibody anti-Runx-2 and anti-Cox-2, at a concentration of 1:200 (Santa Cruz Biotechnology, Santa Cruz, USA). Sections were incubated with biotin conjugated secondary antibody anti-rabbit IgG (Vector Laboratories, Burlingame, CA, USA) in PBS (30 min.) and avidin-biotin complex conjugated to peroxidase (Vector Laboratories, Burlingame, CA, USA) (30 min.). A solution of 3-3'-diaminobenzidine solution (0.05%) and Harris hematoxylin were applied. The immunoexpression of Runx-2 and Cox-2 was assessed both qualitatively (presence and location of the immunomarkers) and quantitatively in five predetermined fields inside the defect using a light microscopy (Leica Microsystems AG, Wetzlar, Germany)

according to a previously described scoring scale from 1 to 4 (1 = absent, 2 = weak, 3 = moderate, and 4 = intense) (Fernandes et al., 2017). The analysis was performed by 2 observers (AFS and GCAV) in a blinded way.

### Statistical Analysis

Data were expressed as mean and standard deviation (±SD). Normality of all variable's distribution was evaluated using the Shapiro–Wilk W test. For variables exhibiting normal distribution, comparisons among the groups were made using one-way analysis of variance (ANOVA), with post hoc Tukey Multiple Comparisons test. For variables exhibiting non-normal distribution, Kruskal Wallis tests were used, with post hoc Dunn. It was used the GraphPad Prism version 6.01 to perform the statistics analysis. Values of $p < 0.05$ were considered statistically significant.

## Results

### Disk preparation

Figure 1 depicts the appearance of the disk manufactured in this work.

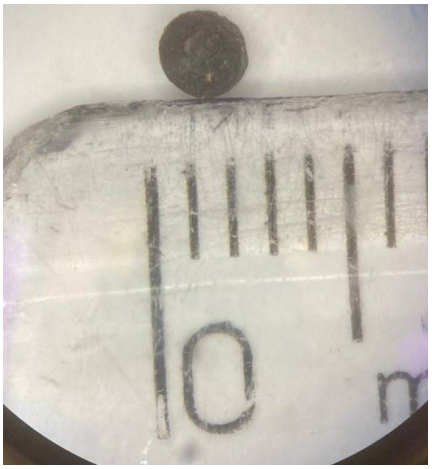

**Figure 1**. Illustrative image of PE scaffold, manufactured by the PE extracted from the marine sponge *Aplysina fulva.*

### SEM

Figure 2 demonstrated the photomicrographies of PE samples in different magnifications. Figures 2A and 2B showed the granular aspect and irregular structure of PE. Moreover, in a higher magnitude, it is possible to observe the smooth surface of the particles, with a heterogenous morphology (Figure 2 C and D).

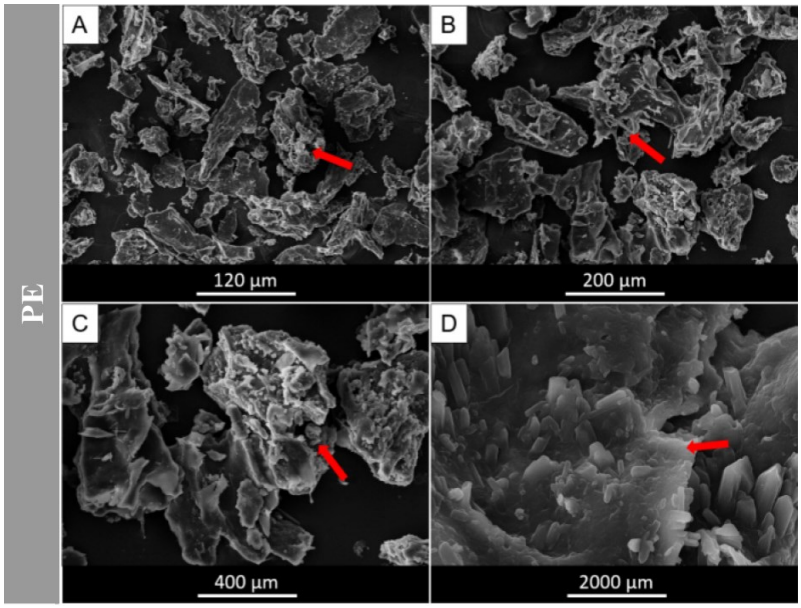


**Figure 2**. SEM representative micrographs of PE extracted from *Aplysina fulva* marine sponge. Red arrows in A-B indicates granular and irregular PE fibers, as well as smooth and heterogeneous PE morphology are depicted in C-D in different magnifications: A 300x; B 500x; C 1000x and D 5000x respectively.

## pH measurements

Figure 3A demonstrated the pH measurements in the periods analyzed for PE and Col samples. After 3 days of immersion in PBS, a slight decrease in the pH was observed for both groups, reaching values of 6.64 and 6.53, respectively. An increase in the pH values was seen along the experimental periods, reaching 8.34 for PE and 6.71 for Col at day 14. However, no significant difference was observed at any experimental point, for both groups.

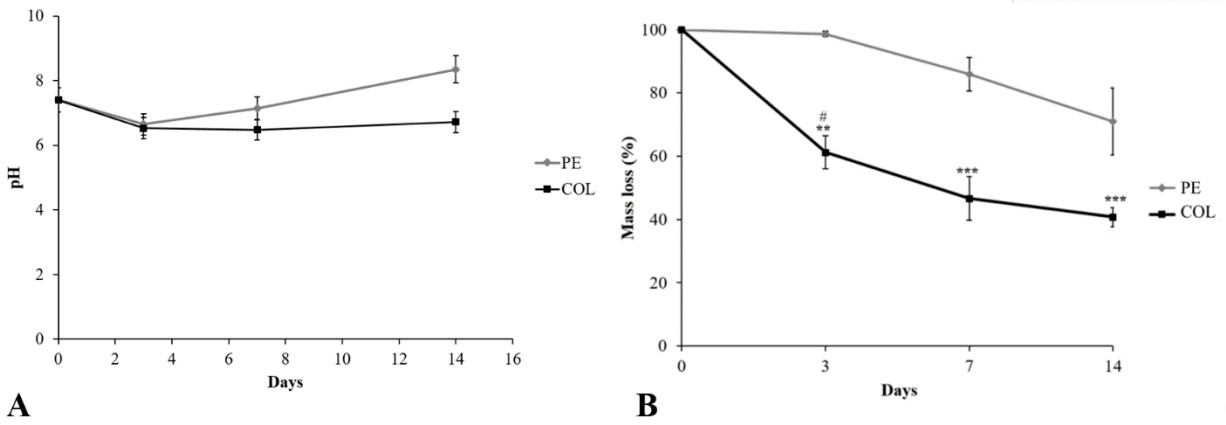


**Figure 3**. A. pH measurements of PBS after contact with PE and COL; B. Mass loss of PE and Col immersed in PBS up to 14 days. Double asterisk indicates $p < 0.01$ and triple asterisk indicates $p < 0.0001$.

## Mass loss assay

Mass loss measurements for PE and Col are depicted in Figure 3B. Protein extract samples did not present any significant decrease along the experimental period (however, the percentage of loss was of 29% comparing the baseline values and values found 14 days after immersion) (Figure 3B). Col samples demonstrated a significant mass loss comparing to the baseline values with the other experimental period of incubation (demonstrating a mass loss of 40 %).

## Cell Viability

Figure 4 demonstrated the cell viability of L929. After 3 days of culture, CG and PE 25 showed significant higher values compared to PE 50 and PE 100. Interestingly, on day 7, CG and PE 50 showed higher values compared to PE 25 and PE 100. On the last period analyzed, cell viability of L929 for CG presented significantly higher values compared to the other groups. Also, PE 25 demonstrated a statistically significant difference compared to PE 50 and PE 100.

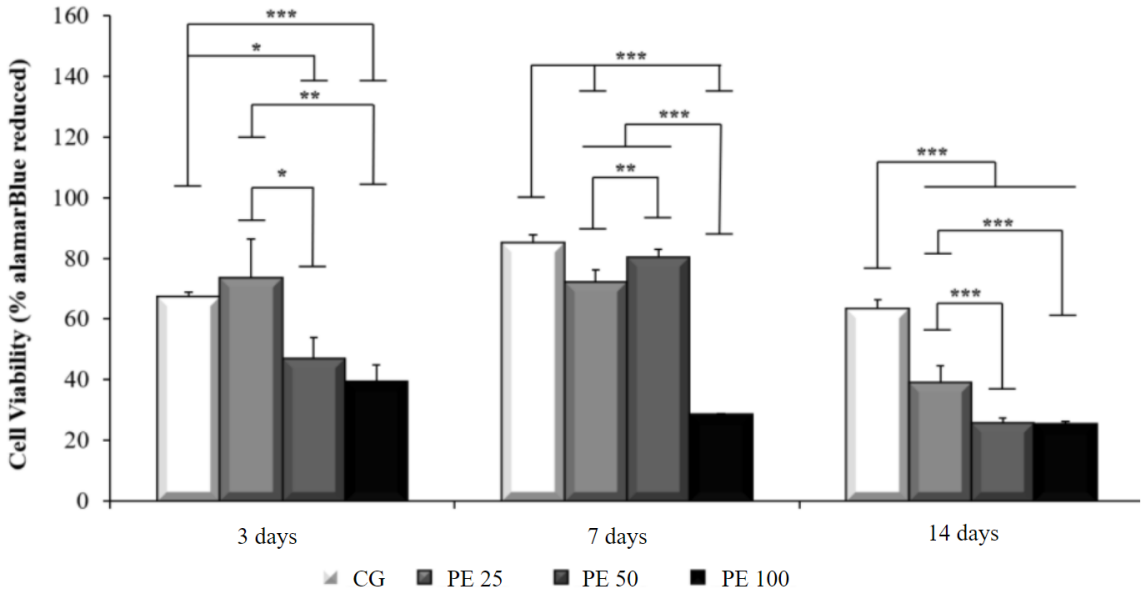


**Figure 4**. Viability of L929 cell line grown in solution containing different PE extracts at different experimental periods (3, 7 and 14 days). One asterisk indicates $p < 0.05$, double asterisk indicates $p < 0.01$, and triple asterisk indicates $p < 0.0001$.

Data about the viability of MC3T3 cells are depicted in Figure 5. The control group demonstrated statistically higher values compared to all PE groups (at all concentrations) on days 3 and 7. At the same experimental periods, cell viability for PE 100 was statistically lower compared to PE at 25 and 50%. A significant difference was observed between PE 25 and 50. On day 14, osteoblast cell viability of CG demonstrated higher values compared to PE 50 and 25. A significant difference was observed comparing PE 50 and PE 25.

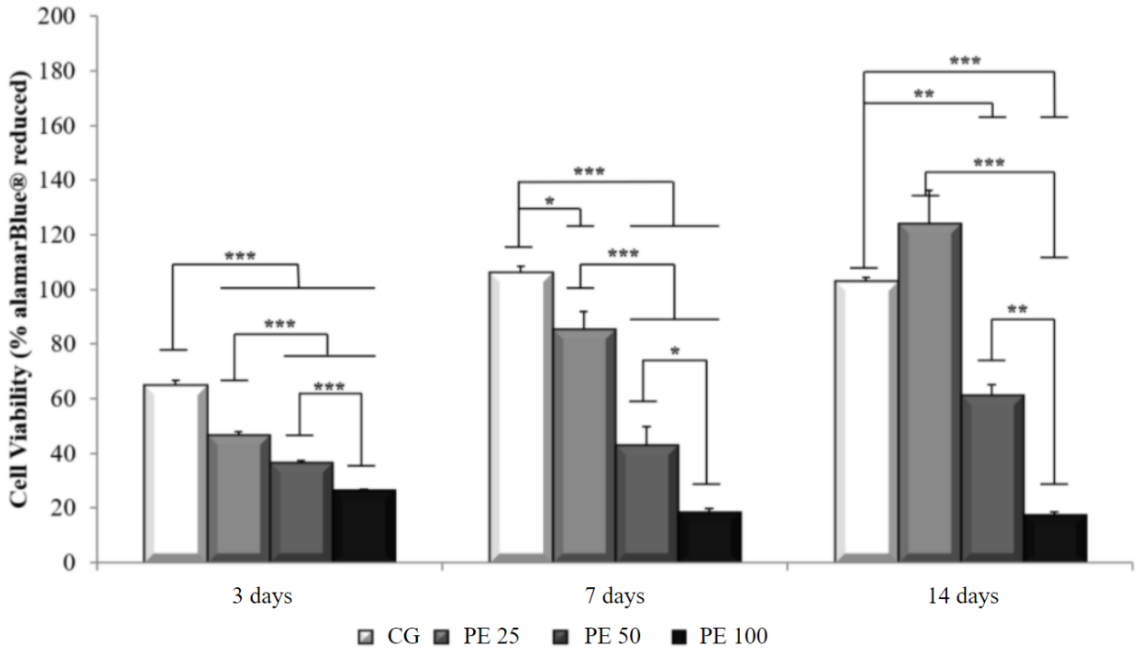


**Figure 5**. Viability of MC3T3 cell line grown in solution containing different PE extracts at different experimental periods (3, 7 and 14 days). Asterisk indicates $p < 0.05$, double asterisk indicates $p < 0,01$, and triple asterisk indicates $p < 0.0001$.

## Comet assay

Figure 6 demonstrates the data of the Comet Assay performed with the samples of PE 25. It is possible to observe that statistically lower values were observed for CG compared to PE 25 at all set points.

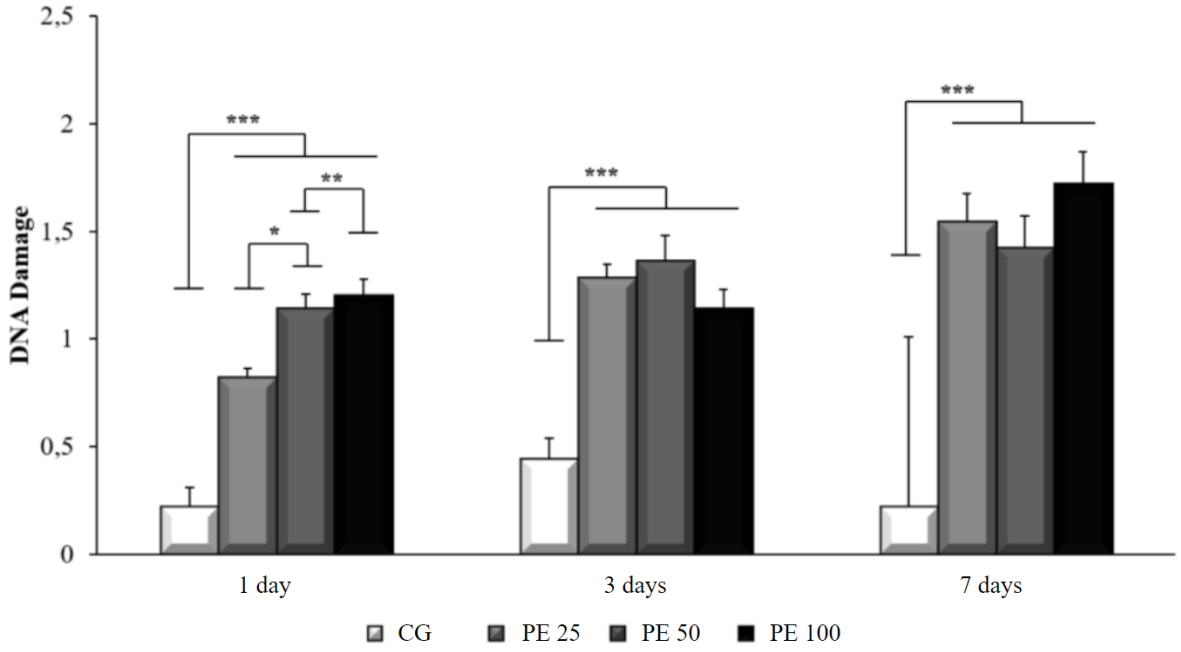


**Figure 6**. Comet Assay using MC3T3 cell line, grown in solution containing different PE extracts. Triple asterisks indicate $p < 0.0001$.

## *In vivo* studies

### Histopathological analysis

Figure 7 represents the histological findings for both experimental groups, 7 days post-surgery. For CG, bone defects were filled mainly by granulation tissue, with some areas of newly formed bone, especially at the periphery (Figures 7 A and 7 B). For PE treated animals, biomaterial particles and granulation tissue could be seen at the region of the defect. Areas of newly formed bone were observed for some animals. There was no inflammatory process or capsule formation between the implant and the edges of defect (Figures 7 C and 7 D).

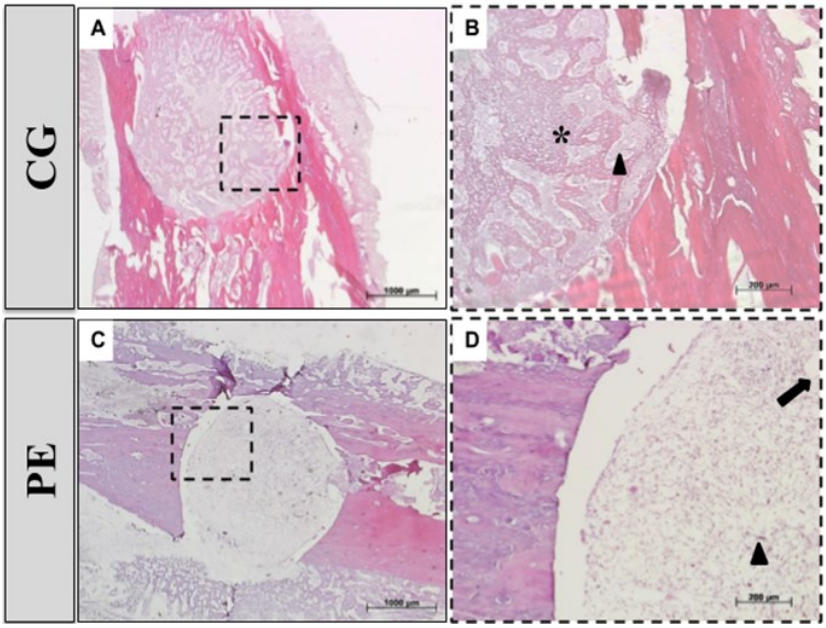


**Figure 7.** Histological sections of the CG and PE groups, 7 days after implantation. *: Newly formed bone; ▲: granulation tissue; ↓: residue of the material. 2.5x magnification (7 A and 7 C) and dashed box indicates the region selected for analysis with 10x magnification (7 B and 7 D). HE staining.

### Immunohistochemistry

For CG, Runx2 immunostaining was observed in the granulation tissue all around the bone defect (Figures 8 A and B). Moreover, for PE, Runx-2 immunostaining was predominantly detected in the granulation tissue at the center of the bone defect and around the particles of the material, 7 days post-surgery (Figures 8 C and D).

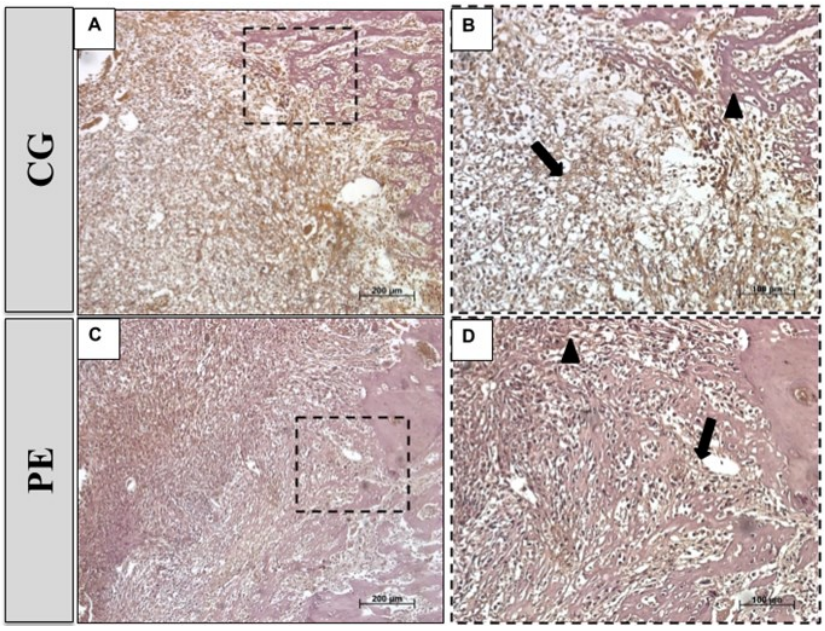


**Figure 8.** Representative photomicrographies for Runx-2 immunohistochemistry of CG (A and B) and PE (C and D) 7 days after surgery. Runx-2 immunostaining (↓). Defect Edge (▲).

Data from the semi-quantitative analysis of Runx-2 immunostaining are demonstrated in Figure 9A. It can be observed that no significant difference was observed between the experimental groups for any immunomarker.

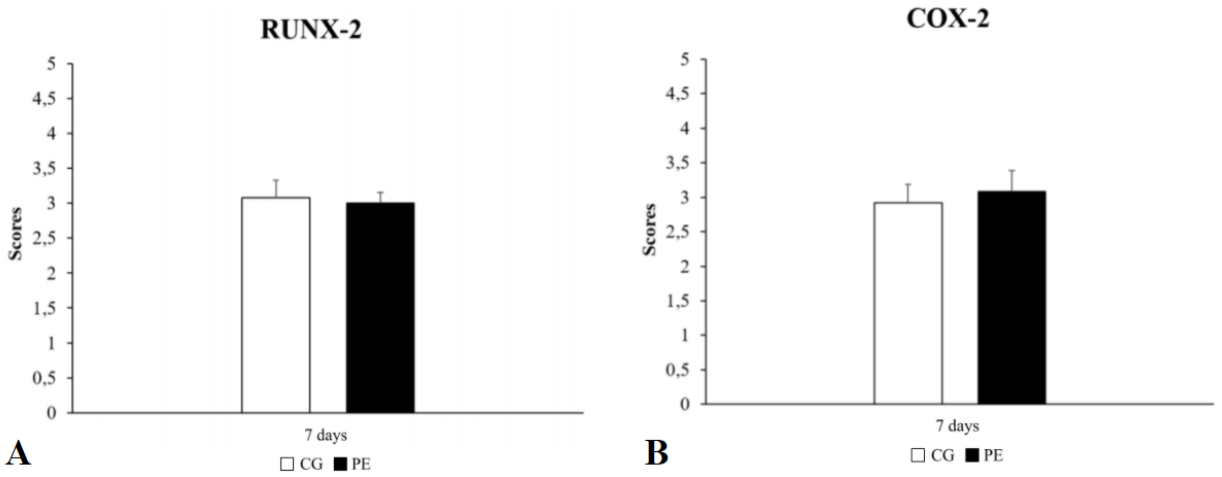


**Figure 9.** (A) Means and standard deviation of Runx-2 immunostaining scores for CG and PE 7 days after surgery. (B) Means and standard deviation of Cox-2 immunostaining scores for CG and PE 7 days after surgery.

Similarly, immunohistochemical evaluation demonstrated that Cox-2 immunostaining was detected mainly in the granulation tissue for CG (Figures 10 A and B). Furthermore, for PE treated animals, Cox2 immunostaining was detected around the material particles, at the center and the edges of the bone defect (Figures 10 C and D).

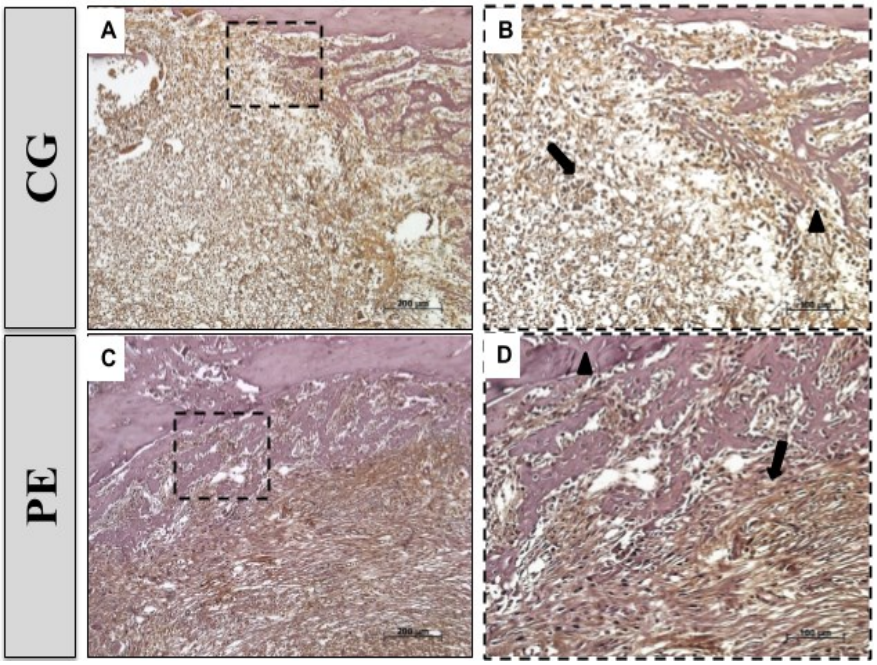


**Figure 10.** Representative photomicrographies for Cox-2 immunohistochemistry of Control group (A and B) and PE (C and D) 7 days after surgery. Cox-2 immunostaining (↓). Defect Edge (▲)

Data from the semi-quantitative analysis of Cox-2 immunostaining are demonstrated in Figure 9B, showing no significant difference between the experimental groups for this immunomarker.

## Discussion

The results demonstrated that PE particles presented a granular and irregular morphology. Moreover, PE samples reached a pH peak of 8.34 and a mass loss of 29% after 14 days of immersion. Higher values for both fibroblast and osteoblast cell viability were found for PE at 25% compared to the other PE groups.

Furthermore, PE 50 and PE 100 demonstrated a significant decrease of viability for both cell lineages and the comet assay showed that PE 25 presented higher values compared to CG. For the *in vivo* experiments, it was possible to observe no inflammatory responses or capsule formation in the PE implanted animals. Also, some degradation of the material was seen. The imunnohistochemistry analysis demonstrated similar Cox-2 and Runx-2 immunostaining for both experimental groups, at day 7.

The protocol of extraction used was efficient to obtain PE from the marine sponges (*Aplysina fulva)*. Furthermore, SEM images showed the irregular aspects of PE particles. Moreover, the dominant organic feature in the PE, was evidenced in the EDS analysis, by the presence of organic compounds such as carbon and oxygen. The pH and mass loss values of PE samples were slightly modified over time, however, with no significant difference. It is known that abrupt modifications of pH induced by the release of ions from biomaterials (both *in vitro* and *in vivo*) can influence cell metabolism and growth, which can delay tissue repair (Pires, Bierhalz, & Moraes, 2015). For example, it has been demonstrated that a significant increase in the pH (up to 14) can be seen when bioglass is immersed in PBS (which releases sodium, calcium, potassium, etc) (Renno et al., 2013). Our results corroborate those found by Magri et al. (2019b) who did not observe any alterations for pH after the incorporation of Col in BG-based materials. In this context, it can be suggested that the lack of significant variation in the pH found in the PE samples, being close to a physiological pH (8.34), may constitute an advantage for supporting cell growth (Magri et al., 2019b).

Also, it was found a mass loss of 29% in the PE samples after 14 days (this behavior could also be seen in the histological analysis). Mass loss evaluation is an important test to measure the index of the material degradation (Félix Lanao, Leeuwenburgh, Wolke, & Jansen, 2011). It is well known that for an improved biological performance of the material to stimulate bone healing, an appropriate degradation rate (matching the capacity of tissue growing into the defects) is necessary, allowing the substitution of the implant by new tissue (Renno et al., 2013; Félix Lanao et al., 2011; Lu, Tang, Oh, Spalazzi, & Dionisio, 2005). Parisi et al. (2019) observed that the inclusion of PE into hydroxypatite samples, increased mass loss of the samples after 14 days. Thus, the PE behavior of the pH and mass loss together may be beneficial to allow cell viability and to induce tissue ingrowth in *in vivo* experimental models and clinical situations.

Cell viability of fibroblasts demonstrated a reduction of 15% and 20% for PE 25 compared to CG, 7 and 14 days of experiments. Also, a significant decrease in cell viability was found for cells cultured in the presence of the 50 and 100% extracts (higher than 30%). For MC3T3 viability, the cells treated with the extract of PE 25 demonstrated a reduction of 20% in the experimental periods of 7 and 14 days, respectively, compared to CG. Also, osteoblast cell viability increased over time in this group (more than 80% from day 3 to day 14). Interestingly, the extracts of 50 and 100% produced a significant decrease of osteoblast cell viability (generally higher than 30%). Kim, Mendis, Rajapakse, Lee, & Kim (2009) demonstrated a lack of cytotoxic effects in incubated MG-63 cells in PE for 3 days. In accord with the ISO 109333-5: 2009, an appropriate material to be used for medical proposals is considered toxic if it induces more than 30% of cell deaths. In this context it can be stated that PE at 25% presented non-cytotoxicity for both fibroblasts and osteoblasts and higher concentrations (50 and 100%) were toxic. Silva et al. (2014), showed that the marine collagen from sponges is biocompatible and stimulates cell viability. Furthermore, the enrichment of hydroxyapatite with PE produced an improvement of the biological performance of HA on the process of bone healing (Parisi et al., 2019). Conversely, the toxic effect found for PE 50 and PE 100 may be explained by the excess of stimulus offered to the cells.

Comet assay is a sensitive and reliable technique for the detection of DNA damage in eukaryotic cells, which evaluates the genotoxicity of therapeutical interventions (Amin, 2019). In the present study, the comet assay was not performed for PE 50 and PE 100 once these groups showed an index of cell death higher than 70 % compared to control group in the viability test following the instructions of (Henderson, Wolfreys, Fedyk, Bourner, & Windebank, 1998). Our results demonstrated that PE 25 produced significant lower values compared to CG. In this study, the comet assay was performed only with the PE 25 due to the non-citotoxicity effects of this extract on cell viability.

Histological findings demonstrated positive results of PE implants into the defect area, with the presence of granulation tissue and no inflammatory response. Exacerbated inflammation and tissue irritation caused by biomaterials are related to rejection and delay in the process of healing (Szponder, Wessely-Szponder, & Sobczyńska-Rak, 2018; Bratlie et al., 2010). Also, some material degradation was observed, which is essential for the stimulation of tissue ingrowth and the production of bone healing (these findings corroborate those found in the evaluation of mass loss). These findings are in line with the results of the current study, which demonstrated that PE implants evoked an inflammatory response, evidencing the *in vivo* biocompatibility.

Tebyanian et al. (2019), demonstrated in a model of cranial bone defect in rabbits, the biocompatibility of Col scaffolds. As far as we know, no other study has evaluated the *in vivo* biocompatibility of PE before.

In order to progress the understanding the interaction of PE and bone tissue, it was evaluated the presence of some markers related to the inflammatory process (Cox-2) and osteoblast differentiation (Runx-2) trough immunohistochemistry analysis. Although the analysis demonstrated the presence of both Cox-2 and Runx-2 in the samples, no difference was observed comparing both groups.

Cox-2 is presented in inflammation sites and produces proinflammatory prostaglandins (Larsson et al., 2015). The lack of difference of Cox-2 immunostaining between both experimental groups (corroborating the histological findings), indicates that PE did not produce any inflammatory reaction on bone tissues. Moreover, Runx-2 is a key factor for mesenchymal progenitor differentiation into osteoblast, resorption and remodeling of bone tissue by osteoclasts respectively (Anandarajah, & Schwarz, 2009). The similar results observed between both groups for Runx-2 immunostaining may be possibly related to the early experimental period evaluated in the present study, which can be considered as the end of the acute phase of repair. Similarly, Magri et al. (2019a) demonstrated no effect on Runx2 immunostaining in cranial bone defects treated with Col.

Despite all the positive results of the material used, further *in vivo* studies are necessary using long-term evaluation to investigate the effects of the chronic implantation of PE samples into bone tissue.

## Conclusion

PE or marine sponge Col has been emerging as a promising alternative from Col derived from other sources such as bovine collagen and other marine collagen. The present study demonstrated that PE with the dissolution of 25% had no cytotoxicity or genotoxicity effect in the *in vitro* studies. Furthermore, the *in vivo* experiments demonstrated that no inflammatory response or capsule formation in the PE treated animals, with degradation of the material. Taken together, all the results suggest that PE is biocompatible and present non-citotoxicity in the *in vitro* studies (at a lower concentration) and in the *in vivo* studies and can be considered as an alternative source of Col for tissue engineering proposals. Future research should focus on investigating the effects of PE on long term periods in animal bone defect model.

## References

Amin, D. M. (2019). Role of copeptin as a novel biomarker of bisphenol A toxic effects on cardiac tissues: biochemical, histological, immunohistological, and genotoxic study. *Environmental Science and Pollution Research International*, *26*(35), 36037-36047. DOI: http://dx.doi.org/10.1007/s11356-019-06855-8

Anandarajah, A. P., & Schwarz, E. M. (2009). Bone loss in the spondyloarthropathies: Role of osteoclast, RANKL, RANK and OPG in the spondyloarthropathies. In C. López-Larrea, R. Díaz-Peña (Eds), *Molecular Mechanisms of Spondyloarthropathies. Advances in Experimental Medicine and Biology* (Vol. 649, p. 85-99). New York, NY: Springer. DOI: http://dx.doi.org/10.1007/978-1-4419-0298-6_6

Assis, L., Moretti, A. I. S., Abrahão, T. B., Souza, H. P., Hamblin, M. R., & Parizotto, N. A. (2013). Low-level laser therapy (808 nm) contributes to muscle regeneration and prevents fibrosis in rat tibialis anterior muscle after cryolesion. *Lasers in Medical Science*, *28*(3), 947-955. DOI: http://dx.doi.org/10.1007/s10103-012-1183-3

Bratlie, K. M., Dang, T. T., Lyle, S., Nahrendorf, M., Weissleder, R., Langer, R., & Anderson, D. G. (2010). Rapid biocompatibility analysis of materials via in vivo fluorescence imaging of mouse models. *PloS ONE*, *5*(4), e10032. DOI: http://dx.doi.org/10.1371/journal.pone.0010032

Cicciù, M., Cervino, G., Herford, A. S., Famà, F., Bramanti, E., Fiorillo, L., ... Laino, L. (2018). Facial bone reconstruction using both marine or non-marine bone substitutes: Evaluation of current outcomes in a systematic literature review. *Marine Drugs*, *16*(1), 27. DOI: http://dx.doi.org/10.3390/md16010027

Colchester, A. C. F., & Colchester, N. T. H. (2005). The origin of bovine spongiform encephalopathy: the human prion disease hypothesis. *The Lancet*, *366*(9488), 856-861. DOI: http://dx.doi.org/10.1016/S0140-6736(05)67218-2

Chattopadhyay, S., & Raines, R. T. (2014). Collagen-based biomaterials for wound healing. *Biopolymers*, *101*(8), 821-833. DOI: http://dx.doi.org/10.1002/bip.22486

Davison-Kotler, E., Marshall, W. S., & García-Gareta, E. (2019). Sources of collagen for biomaterials in skin wound healing. *Bioengineering*, *6*(3), 56. DOI: http://dx.doi.org/10.3390/bioengineering6030056

Felician, F. F., Xia, C., Qi, W., & Xu, H. (2018). Collagen from marine biological sources and medical applications. *Chemistry & Biodiversity*, *15*(5), e1700557. DOI: http://dx.doi.org/10.1002/cbdv.201700557

Félix Lanao, R. P., Leeuwenburgh, S. C. G., Wolke, J. G. C., & Jansen, J. A. (2011). In vitro degradation rate of apatitic calcium phosphate cement with incorporated PLGA microspheres. *Acta Biomaterialia*, *7*(9), 3459-3468. DOI: http://dx.doi.org/10.1016/j.actbio.2011.05.036

Fernandes, K. R., Magri, A., Kido, H. W., Parisi, J. R., Assis, L., Fernandes, K., ... Renno, A. (2017). Biosilicate/PLGA osteogenic effects modulated by laser therapy: In vitro and in vivo studies. *Journal of photochemistry and photobiology. B, Biology*, *173*, 258–265. DOI: https://doi.org/10.1016/j.jphotobiol.2017.06.002

Gabbai-Armelin, P. R., Souza, M.T., Kido, H.W., Tim, C. R., Magri, A. M. P., Fernandes, K. R., ... Renno, A. C. M. (2015). Effect of a new bioactive fibrous glassy scaffold on bone repair. *Journal of Materials Science: Materials in Medicine*, *26*, 177. DOI: http://dx.doi.org/10.1007/s10856-015-5516-1

Garavello-Freitas, I., Baranauskas, V., Joazeiro, P. P., Padovani, C. R., Dal Pai-Silva, M., & da Cruz-Höfling, M. A. (2003). Low-power laser irradiation improves histomorphometrical parameters and bone matrix organization during tibia wound healing in rats. *Journal of Photochemistry and Photobiology B, Biology*, *70*(2), 81-89. DOI: http://dx.doi.org/10.1016/s1011-1344(03)00058-7

Green, D., Howard, D., Yang, X., Kelly, M., & Oreffo, R. O. C. (2003). Natural marine sponge fiber skeleton: a biomimetic scaffold for human osteoprogenitor cell attachment, growth, and differentiation. *Tissue engineering*, *9*(6), 1159-1166. DOI: http://dx.doi.org/10.1089/10763270360728062

Green, D. W., Lee, J.-M., & Jung, H.-S. (2015). Marine structural biomaterials in medical biomimicry. *Tissue Engineering Part B: Reviews*, *21*(5), 438-450. DOI: http://dx.doi.org/10.1089/ten.TEB.2015.0055

Hägg, P., Väisänen, T., Tuomisto, A., Rehn, M., Tu, H., Huhtala, P., ... Pihlajaniemi, T. (2001). Type XIII collagen: a novel cell adhesion component present in a range of cell-matrix adhesions and in the intercalated discs between cardiac muscle cells. *Matrix Biology*, *19*(8), 727-742. DOI: http://dx.doi.org/10.1016/s0945-053x(00)00119-0

Henderson, L., Wolfreys, A., Fedyk, J., Bourner, C., & Windebank, S. (1998). The ability of the Comet assay to discriminate between genotoxins and cytotoxins. *Mutagenesis*, *13*(1), 89-94. DOI: http://dx.doi.org/10.1093/mutage/13.1.89

Hoyer, B., Bernhardt, A., Heinemann, S., Stachel, I., Meyer, M., & Gelinsky, M. (2012). Biomimetically mineralized salmon collagen scaffolds for application in bone tissue engineering. *Biomacromolecules*, *13*(4), 1059-1066. DOI: http://dx.doi.org/10.1021/bm201776r

Iwatsubo, T., Kishi, R., Miura, T., Ohzono, T., & Yamaguchi, T. (2015). Formation of hydroxyapatite skeletal materials from hydrogel matrices via artificial biomineralization. *The Journal of Physical Chemistry. B*, *119*(28), 8793-8799. DOI: http://dx.doi.org/10.1021/acs.jpcb.5b03181

Khan, R., & Khan, M. H. (2013). Use of collagen as a biomaterial: An update. *Journal of Indian Society of Periodontology* , *17*(4), 539-542. DOI: http://dx.doi.org/10.4103/0972-124X.118333

Kido, H. W., Oliveira, P., Parizotto, N. A., Crovace, M. C., Zanotto, E. D., Peitl-Filho, O., ... Renno, A. C. M. (2013). Histopathological, cytotoxicity and genotoxicity evaluation of Biosilicate® glass-ceramic scaffolds. *Journal of Biomedical Materials Research. Part A*, *101*(3), 667-673. DOI: http://dx.doi.org/10.1002/jbm.a.34360

Kim, M.-M., Mendis, E., Rajapakse, N., Lee, S.-H., & Kim, S.-K. (2009). Effect of spongin derived from *Hymeniacidon sinapium* on bone mineralization. *Journal of Biomedical Materials Research. Part B, Applied Biomaterials*, *90B*(2), 540-546. DOI: http://dx.doi.org/10.1002/jbm.b.31315

Larsson, K., Kock, A., Idborg, H., Henriksson M. A., Martinsson, T., Johnsen, J. I., ... Jakobsson, P.-J. (2015). COX/mPGES-1/PGE2 pathway depicts an inflammatory-dependent high-risk neuroblastoma subset. *Proceedings of the National Academy of Sciences of the United States of America*, *112*(26), 8070-8075. DOI: http://dx.doi.org/10.1073/pnas.1424355112

Lim, Y.-S., Ok, Y.-J., Hwang, S.-Y., Kwak, J.-Y., & Yoon, S. (2019). Marine collagen as a promising biomaterial for biomedical applications. *Marine Drugs*, *17*(8), 467. DOI: http://dx.doi.org/10.3390/md17080467

Lu, H. H., Tang, A., Oh, S. C., Spalazzi, J. P., & Dionisio, K. (2005). Compositional effects on the formation of a calcium phosphate layer and the response of osteoblast-like cells on polymer-bioactive glass composites. *Biomaterials*, *26*(32), 6323-6334. DOI: http://dx.doi.org/10.1016/j.biomaterials.2005.04.005

Magri, A. M. P., Fernandes, K. R., Kido, H. W., Fernandes, G. S., Fermino, S. S., Gabbai-Armelin, P. R., ... Rennó, A. C. M. (2019a). Bioglass/PLGA associated to photobiomodulation: effects on the healing process in an experimental model of calvarial bone defect. *Journal of Materials Science. Materials in Medicine*, *30*(9), 105. DOI: http://dx.doi.org/10.1007/s10856-019-6307-x

Magri, A. M. P., Fernandes, K. R., Assis, L., Kido, H. W., Avanzi, I. R., Medeiros, M. C., ... Rennó, A. C. M. (2019b). Incorporation of collagen and PLGA in bioactive glass: in vivo biological evaluation. *International Journal of Biological Macromolecules*, *134*, 869-881. DOI: http://dx.doi.org/10.1016/j.ijbiomac.2019.05.090

Müller, W. E., Krasko, A., Skorokhod, A., Bünz, C., Grebenjuk, V. A., Steffen, R., ... Schröder, H. C. (2002). Histocompatibility reaction in tissue and cells of the marine sponge Suberites domuncula in vitro and in vivo: central role of the allograft inflammatory factor 1. *Immunogenetics*, *54*(1), 48-58. DOI: http://dx.doi.org/10.1007/s00251-002-0441-0

Parisi, J. R., Fernandes, K. R., Avanzi, I. R., Dorileo, B. P., Santana, A. F., Andrade, A. L., ... Renno, A. C. M. (2019). Incorporation of collagen from marine sponges (Spongin) into hydroxyapatite samples: characterization and in vitro biological evaluation. *Marine Biotechnology*, *21*(1), 30-37. DOI: http://dx.doi.org/10.1007/s10126-018-9855-z

Pires, A. L. R., Bierhalz, A. C. K., & Moraes, Â. M. (2015). Biomateriais: Tipos, aplicações e mercado. *Quimica Nova, 38*(7), 957-971. DOI: http://dx.doi.org/10.5935/0100-4042.20150094

Pozzolini, M., Scarfì, S., Gallus, L., Castellano, M., Vicini, S., Cortese, K., ... Giovine, M. (2018). Production, characterization and biocompatibility evaluation of collagen membranes derived from marine sponge *Chondrosia reniformis* Nardo, 1847. *Marine Drugs*, *16*(4), 111. DOI: http://dx.doi.org/10.3390/md16040111

Renno, A. C. M., Bossini, P. S., Crovace, M. C., Rodrigues, A. C. M., Zanotto, E. D., & Parizotto, N. A. (2013). Characterization and in vivo biological performance of biosilicate. *BioMed Research International*, *2013,* 141427. DOI: http://dx.doi.org/10.1155/2013/141427

Silva, T. H., Moreira-Silva, J., Marques, A. L. P., Domingues, A., Bayon, Y., & Reis, R. L. (2014). Marine origin collagens and its potential applications. *Marine Drugs*, *12*(12), 5881-5901. DOI: http://dx.doi.org/10.3390/md12125881

Swatschek, D., Schatton, W., Kellermann, J., Müller, W. E. G., & Kreuter, J. (2002). Marine sponge collagen: isolation, characterization and effects on the skin parameters surface-pH, moisture and sebum. *European Journal of Pharmaceutics and Biopharmaceutics*, *53*(1), 107-113. DOI: http://dx.doi.org/10.1016/s0939-6411(01)00192-8

Szponder, T., Wessely-Szponder, J., & Sobczyńska-Rak, A. (2018). The neutrophil response to rabbit antimicrobial extract after implantation of biomaterial into a bone/cartilage defect. *In vivo*, *32*(6), 1345-1351. DOI: http://dx.doi.org/10.21873/invivo.11385

Tebyanian, H., Norahan, M. H., Eyni, H., Movahedin, M., Mortazavi, S. M. J., Karami, A., ... Baheiraei, N. (2019). Effects of collagen/β-tricalcium phosphate bone graft to regenerate bone in critically sized rabbit calvarial defects. *Journal of Applied Biomaterials & Functional Materials*, *17*(1), 2280800018820490. DOI: http://dx.doi.org/10.1177/2280800018820490

Wang, B., Dong, J., Zhou, X., Lee, K. J., Huang, R., Zhang, S., & Liu, Y. (2009). Nucleosides from the marine sponge *Haliclona* sp. *Zeitschrift fur Naturforschung. C, 64*(1-2), 143-148. DOI: http://dx.doi.org/10.1515/znc-2009-1-223

Ylönen, R., Kyrönlahti, T., Sund, M., Ilves, M., Lehenkari, P., Tuukkanen, J., & Pihlajaniemi, T. (2005). Type XIII collagen strongly affects bone formation in transgenic mice. *Journal of Bone and mineral Research, 20*(8), 1381-1393. DOI: http://dx.doi.org/ 10.1359/JBMR.050319